Quantitative lipidomics reveals lipid perturbation in the liver of fatty liver hemorrhagic syndrome in laying hens

Manhua You,* Shaobo Zhang,* Youming Shen,† Xinghua Zhao,* Ligong Chen,* Juxiang Liu,* and Ning Ma *,[1]

*College of Veterinary Medicine, Veterinary Biological Technology Innovation Center of Hebei Province, Hebei Agricultural University, Baoding 071001, Hebei, China; and †Research Institute of Pomology, Chinese Academy of Agricultural Sciences, Xingcheng 125100, China

ABSTRACT Fatty liver hemorrhagic syndrome (**FLHS**) is a metabolic disease that causes decreased egg production and even death in laying hens, which brings huge economic losses to the poultry industry. However, the pathogenesis of FLHS is unclear. The purpose of the present study was to identify the changes in lipid profile and the lipid species related to FLHS. In the present study, the FLHS disease model in Chinese commercial Jing Fen laying hens was induced by a high-energy low-protein diet. A lipidomics approach based on ultra-performance liquid chromatography-mass spectrometry coupled with multivariate statistical analysis was performed for the qualitative and quantitative analyses of the liver lipids. The results showed that a total of 29 lipid subclasses, including 1,302 lipid species, were detected and identified. Among them, the proportions of phosphatidylserine (Control/FLHS, 33.1% vs. 29.1%), phosphatidylethanolamine (22.7% vs. 15.5%), phosphatidylcholine (15.7% vs. 11.7%) and phosphatidylinositol (7% vs. 6%) were reduced, while triacylglycerol (7.1% vs. 18.3%) and diglyceride (3.9% vs. 11.7%) were increased. Between the Control and FLHS groups, distinct changes in lipid profile were observed in the score plots of principal component analysis and orthogonal partial least squares discriminant analysis. Twelve differential lipid species mainly involved in glycerophospholipid metabolism and linoleic acid metabolism were identified and considered to be related to the pathogenesis of FLHS. Fatty acid chain length and unsaturation were reduced, while the mRNA levels of elongation of very long chain fatty acids-2 (ELOVL2) were increased in the liver of laying hens with FLHS. Collectively, this study characterized the liver lipid profile and explored the changes in lipid species related to FLHS, which provided insights into the pathogenesis of FLHS from the view of lipid metabolism.

Key words: fatty liver hemorrhagic syndrome, laying hens, lipidomics, lipid pathway, lipid profile

2023 Poultry Science 102:102352
https://doi.org/10.1016/j.psj.2022.102352

INTRODUCTION

Fatty liver hemorrhage syndrome (**FLHS**) is the most non-communicable disease of laying hens. There is a prevalence of FLHS of up to 16% worldwide, which affects feed intake, egg production, egg weight, and even laying hen mortality, resulting in huge economic loss for the layer industry (Rozenboim et al., 2016; Cheng et al., 2022). Previous studies indicated that FLHS is a kind of nutritional and metabolic disease, and the main manifestation of FLHS is excessive lipid deposition in the liver. Notably, lipid accumulates excessively in the liver cells of the laying hens with FLHS, damaging the normal function of the liver. It even leads to the rupture of hepatocytes, which eventually leads to intrahepatic bleeding and the death of laying hens (Shini et al., 2019). However, the lipid metabolic changes caused by FLHS have not been fully identified and characterized. As the primary organ for lipid metabolism, the liver contains numerous classes of lipids. These lipids possess diverse biological functions such as cellular signaling, energy metabolism, and regulation factor of diseases (Meikle et al., 2014). Therefore, the comprehensive investigation of lipid species in the liver may provide new evidence and perspective for elucidating the pathogenesis of FLHS.

Lipidomics uses high-throughput analysis technology to analyze the structure and function of lipids in cells, tissues or organisms, which can promote the understanding of the multiple biological functions of lipids. As a powerful methodology, lipidomics is widely applied in

Received August 25, 2022.
Accepted November 15, 2022.

[1]Corresponding author: maning9618@163.com

many metabolic disease pathogenesis, diagnosis, and drug development, such as fatty liver disease, diabetes, and cardiovascular disease (Yang et al., 2016; Ding and Rexrode, 2020). The researchers found that diacylglycerol, triacylglycerol (**TG**), and hepatic free cholesterol increased significantly, while total phosphatidylcholine decreased in the patients with nonalcoholic fatty liver disease (**NAFLD**) and nonalcoholic steatohepatitis (**NASH**) via lipidomics studies (Puri et al., 2007). With the application of comprehensive lipid analysis in the liver, Chiappini et al. found 32 lipid features discriminating NASH from normal liver and nonalcoholic fatty liver, which might be the potential biomarkers for NASH diagnosis (Chiappini et al., 2017). Hepatic lipidomics analysis also provided evidence that cereal β-glucan could improve lipid metabolic patterns and regulate 13 lipid species (most of which related to glycerophospholipids metabolism and glycerolipid metabolism) in NAFLD mice induced by a Western diet, which elucidated the underlying mechanisms of cereal β-glucan on NAFLD prevention (Liu et al., 2021). These studies indicated that lipidomics is an attractive power approach and can be employed to determine and identify lipid biomarkers. However, as far as we know, there are no reports about the lipid metabolism associated with FLHS in laying hens with the application of lipidomics.

Nuclear Magnetic Resonance (**NMR**), gas chromatography coupled to mass spectrometry (**GC-MS**), and liquid chromatography coupled with mass spectrometry (**LC-MS**) are the three main detection methods of the lipidomics platforms. NMR does not damage the biological samples and has good repeatability (Li et al., 2017). However, its low sensitivity, low resolution, and high cost limit its use in experiments (Emwas et al., 2019). Although GC-MS has high sensitivity and high resolution, its samples need to be derivatized, leading to longer sample preparation time (Eylem et al., 2022). Compared with the above detection methods, LC-MS has higher sensitivity and resolution and is not restricted by derivatization, volatility, and other conditions (Gika et al., 2014). Electrospray ionization (**ESI**), an ionization technology, has been widely used to LC-MS analysis and employed in lipidomics studies recently. Through hepatic lipidomics, Feng et al. investigated the underlying mechanism of tangeretin in antiobesity and cholesterol-lowering, and found that some lipid biomarkers such as fatty acids, ceramides, and cholesteryl esters were responsible for the beneficial effects such as the reduction of weight gain and cholesterol and the improvement of liver steatosis (Feng et al., 2020). With the application LC-ESI-MS based lipidomics, Wang et al. found that the development of NASH from NAFLD was closely related to the aberrant metabolism of phospholipids (Wang et al., 2021). Therefore, lipidomics is an essential tool for investigating the dysregulation of lipid metabolism. However, so far, no study applied lipidomics in the pathogenesis of FLHS.

The present study aimed to identify the changes in liver lipid profile and lipid species related to FLHS in laying hens. Lipids associated with FLHS were screened and investigated through the application of UHPLC Q-Exactive MS-based liver lipidomics combined with multivariate statistical analysis and pathway analysis. These findings were helpful for us to understand FLHS and provide new insights into the pathogenesis of FLHS from the perspective of lipid metabolism.

MATERIALS AND METHODS

Chemicals

Methanol, acetonitrile, and isopropanol of mass-grade were purchased from Thermo Fisher Scientific (Massachusetts). Formic acid was obtained from Fluka (Steinheim, Germany). Ammonium formate and Tert-butyl methyl ether (**MTBE**) were purchased from Sigma-Aldrich (St. Louis, MO). The internal standard of SPLASH LIPIDOMIX MASS SPRC STANDARD was from Avanti Polar Lipids Inc (Alabama, AL).

Experiment Animals

The experimental procedures were reviewed and approved by the Institutional Animal Care and Use Committee of Hebei Agricultural University (Approval No. 2021066) and carried out in accordance with the Guidelines of the Care and Use of Laboratory Animals of China. In the present study, twenty healthy 90-day-old Chinese commercial Jing Fen laying hens were used. All the laying hens were in cages (2 hens per cage) with ad libitum access to water and feed. The hens were housed at 22 ± 3℃, and the relative humidity was controlled at 50% ± 10%. The lighting time was maintained daily from 6:00 am to 10:00 pm. FLHS was induced by the high-energy low-protein (**HELP**) diet in laying hens according to previous studies (Gao et al., 2019; Meng et al., 2021). All the laying hens had a 2-wk adjustment period before the experiment. The hens were randomly divided into 2 treatment groups (10 laying hens for each treatment, n = 10): the Control group, in which the laying hens were fed with a standard diet; the FLHS group, in which the laying hens were fed with HELP diet. The detailed composition and nutritional level of the standard diet and HELP diet were provided in Supplementary Table 1. The laying hens in the FLHS group were administrated with the HELP diet for 48 successive days. At the end of the experiment, all the laying hens were fasted for 12 h and then euthanized. Blood samples were collected and separated by centrifugation (4,000 *g*, for 10 min at 4°C) to obtain serum for lipid parameters analysis including total cholesterol (**TCH**), TG, alanine transaminase (**ALT**), aspartate aminotransferase (**AST**), low-density lipoprotein (**LDL**) and high-density lipoprotein (**HDL**). The liver samples were fixed with formalin, embedded in paraffin, cut into 5 μm slices, and then subjected to standard hematoxylin and eosin (H&E). Frozen liver sections were stained with oil red O to examine lipid droplets. The histopathological changes were observed by CX31 biological microscope (Olympus Corporation, Tokyo, Japan). Meanwhile, parts of the

liver tissue were snap-frozen in liquid nitrogen and stored at −80°C for lipidomic analysis.

Quantitative Real-time PCR (qRT-PCR) Analysis

The liver tissue of laying hens was taken out of the refrigerator at −80°C, and the total RNA was isolated from the liver tissue by TaKaRa kit (Beijing, China). A PrimeScript RT reagent kit (TaKaRa, Beijing, China) is used to reverse-transcribe it into cDNA. Gene expression levels of carnitine palmitoyltransferase-1 (**CPT1**), fatty acid desaturase-like 1 (**FADS1**), elongation of very long chain fatty acids-2 (**ELOVL2**), and elongation of very long chain fatty acids-5 (**ELOVL5**) were detected by qRT-PCR in a CFX Connect Real-Time System (CFX96, Bio-Rad, CA) with the SYBR Green Premix. The relative expression of each gene was calculated by the $2^{-\Delta\Delta CT}$ method. The primers of the detected genes were provided in Supplementary Table 2.

Liver Sample Preparation for Lipidomic Analysis

For lipid extraction, the lipids in the liver were extracted according to the methyl tert-butyl ether (**MTBE**) method (Matyash et al., 2008). Six liver samples harvested from the Control and FLHS groups were randomly selected and thawed at room temperature, and then accurately weighed. In EP tubes, the liver samples (30 mg) were spiked with 20 μL internal lipid standards, and then 200 μL water and 240 μL methanol were added. After mixing, the samples were homogenized by an MP homogenizer (24×2, 6.0 M/S, 60 s, twice). Then, 800 μL of MTBE was added and the mixture was sonicated for 20 min at 4°C followed by sitting still for 30 min at room temperature. The mixtures were subsequently centrifuged at 14,000 *g* for 15 min at 10°C. Next, the upper layer was obtained and dried under nitrogen. After drying, the lipid extracts were reconstituted in 200 μL of 90% isopropanol/acetonitrile, and the reconstituted samples were centrifuged at 14,000 *g* for 15 min. Finally, the supernatant was collected and 3 μL of the sample was injected into UHPLC Q-Exactive MS for lipidomics analysis. Three quality control (**QC**) samples were prepared by pooling 10 μL of each sample and analyzed under the same procedure to assess the method repeatability and system stability.

Lipidomics Data Acquisition and Processing

Lipidomic analysis of liver samples was carried out with the application of a Nexera UHPLC LC-30A system (Shimadzu Corporation, Japan) coupled to Q-Exactive Plus mass spectrometer (Thermo Fisher Scientific). The separation was performed on a reverse phase CSH C18 column (1.7 μm, 2.1 mm × 100 mm, Waters) at a flow rate of 300 μL/min under 45°C. Mobile phase A consisted of acetonitrile−water (6:4, v/v) with 0.1% formic acid and 0.1 mM ammonium formate, and mobile phase B was acetonitrile−isopropanol (1:9, v/v) with 0.1% formic acid and 0.1 mM ammonium formate. The mobile phase gradient was as follows: 0 min, 30% B; 0 to 2 min, 30% B; 2 to 25 min, 30 to 100% B; 25 to 35 min, 5% B for equilibrating. The autosampler temperature was set at 10°C.

Mass spectra data were acquired by Q-Exactive Plus mass spectrometer with ESI source operated in positive and negative modes, respectively. ESI parameters were optimized as follows: source temperature, 300°C; capillary temperature, 350°C; the ion spray voltage, 3000 V; S-Lens RF Level, 50%; sheath gas flow rate 45 arb; aux gas flow rate15 arb; sweep gas flow rate 1 arb and the scan range, 200 to 1800 mass-to-charge ratio (**m/z**). To further identify lipids, mass charge ratio of lipid species and lipid fragments was collected. Tandem mass spectrometry (**MS/MS**) scan was carried out to acquire ten fragments of lipid species after a full scan using higher energy collisional dissociation. The resolution of MS was 70,000 at m/z of 200 and that of MS/MS was 17 500 at m/z of 200.

Multivariate Data Analysis, Pathway Analysis and Statistical Analysis

For the raw data, LipidSearch software (Version 4.2, Thermo Scientific) was used to extract and identify the peaks of lipids with the main parameters as follows: precursor tolerance, 5 ppm; product tolerance, 5 ppm and product ion threshold, 5%. Peak alignment, retention time correction and extraction of peak area were also performed by LipidSearch software. Meanwhile, the ion peak with a value of >50% missing from the group was removed. After normalization and integration using the Perato scaling method, the final dataset was imported into SIMPCA (version 16.1, Umetrics, Umea, Sweden) for a multivariate statistical analysis. Principal component analysis (**PCA**) and orthogonal partial least squares discriminant analysis (**OPLS-DA**) were carried out to visualize the distribution and the grouping of the liver samples from the Control and FLHS group (n = 6). In order to evaluate the robustness of the OPLS-DA model, the permutation test with 200 times was conducted. After that, the value of variable importance in the projection (**VIP**) from OPLS-DA models was calculated. The comparison of the variables between the Control and FLHS group was carried out by student's t-test followed by SPSS 16.0 (Version 16.0, SPSS Inc., Chicago), and the *P*-value was obtained. With VIP > 1 and *P*-value < 0.05, the lipid species were considered significant and selected. Hierarchical clustering, correlation analysis, and heatmap analysis were performed and visualized by the R package. Pathway analysis of the lipid species was carried out using MetaboAnalyst 5.0 with the using of the pathway library of *Gallus gallus* in the KEGG database (Pang et al., 2022).

The data were presented as the mean ± standard deviation (**SD**). Statistical analysis was performed using

SPSS 16.0 (SPSS Inc., Chicago, IL). Statistical differences between the Control group and FLHS group was analyzed using Student's t test. $P < 0.05$ was considered statistically significant.

RESULTS

Hepatic Lipid Composition

In order to validate the FLHS disease model, serum lipid parameters analysis and liver pathological examination by HE and oil red O staining were firstly carried out. The results of blood lipids and hepatic histopathology were provided in Supplementary Table 3 and Supplementary Figure 1 (Meng et al., 2021). Compared with the Control, the levels of TCH, TG, ALT, AST, and LDL in serum were significantly increased ($P < 0.01$), while HDL was decreased ($P < 0.01$). In addition, hepatic steatosis and lipid accumulation were obviously found in the liver cells from the laying hens in the FLHS group, which were absent in those of the Control group (Supplementary Figure 1). These results indicated that the FLHS model was successfully established by the HELP diet in laying hens.

The typical base peak chromatograms of liver samples in positive and negative modes were shown in Supplementary Figure 2. It was observed that lipids components were generally detected and separated with the current method. A total of 1,302 lipid species, categorized into 29 different lipid subclasses, were identified and annotated from the analyzed liver samples (Table 1). The subclass of TG had the highest number of lipid species at 233, followed by phosphatidylcholine (**PC**, 231) and phosphatidylethanolamine (**PE**, 196). The content percentages of 29 lipid subclasses in the liver from laying hens in Control and FLHS groups were obtained through the application of absolute quantities of lipids. As shown in Figure 1, it was found that TG, phosphatidylserine (**PS**), PE, PC, phosphatidylinositol (**PI**), and diglyceride (**DG**) were the predominant fraction in the liver of laying hens, around 91% of the total lipid. Compared with the Control group, the proportions of PS (Control versus FLHS, 33.1% vs. 29.1%), PE (22.7% vs. 15.5%), PC (15.7% vs. 11.7%), and PI (7% vs. 6%) were reduced in the FLHS group, while TG (7.1% vs. 18.3%) and DG (3.9% vs. 11.7%) were increased in the laying hens with FLHS (Figure 1).

Table. 1. Lipid subclasses of liver from laying hens analyzed by lipidomics.

Lipid subclass	Abbreviation	Number of identified lipid molecules
Acyl Carnitine	AcCa	5
Ceramides	Cer	43
Monogylcosylceramide	CerG1	34
Diglycosylceramide	CerG2	11
Cardiolipin	CL	72
Coenzyme Q	Co	2
Diglyceride	DG	18
Fatty acid	FA	12
Monosialodihexosylganglioside	GM3	24
Lysophosphatidic acid	LPA	2
Lysophosphatidylcholine	LPC	29
Lysophosphatidylethanolamine	LPE	26
Lysophosphatidylglycerol	LPG	10
Lysophosphatidylinositol	LPI	8
Lysophosphatidylserine	LPS	9
Monogalactosyldiacylglycerol	MGDG	20
Phosphatidic acid	PA	5
Phosphatidylcholine	PC	231
Phosphatidylethanolamine	PE	196
Phosphatidylglycerol	PG	27
Phytosphingosine	phSM	2
Phosphatidylinositol	PI	31
Phosphatidylinositol-4-phosphate	PIP	6
Phosphatidylserine	PS	64
Sphingomyelin	SM	62
Sphingosine	So	5
Sulfoquinovosyldiacylglycerol	SQDG	6
Triacylglycerol	TG	233
Wax exters	WE	9

Lipid Profile of FLHS

In order to visualize the group separation and distinguish lipid profile differences, unsupervised PCA was carried out on the liver samples between the Control group and the FLHS group. It was found that the three QC samples were tightly overlapped in the PCA score plot (Figure 2A), indicating the good stability and reliability of the lipidomics analytical method. Moreover, PCA analysis found that the liver samples in the FLHS group were distinguished from those in the Control group, indicating the different patterns of the lipid profiling. To achieve a clear separation and obtain the variables responsible for classification, supervised OPLS-DA was performed (Figure 2B). For the OPLS-DA model, R^2 and Q^2 indicate the explanatory power and predictive ability of the model, respectively. The parameters for the generated OPLS-DA model between the Control and FLHS groups were as follows: $R^2X = 0.60$, $R^2Y = 0.91$, and $Q^2 = 0.61$. It was observed that the FLHS group was clearly separated away from the Control group in the OPLS-DA score plot (Figure 2B), suggesting there was a disorder of lipid homeostasis in laying hens in the FLHS group caused by the HELP diet. Moreover, in order to avoid the overfitting of the OPLS-DA, the permutation test (200 times) was conducted. The OPLS-DA model robustness is reflected by the intercept value of Q^2, and there is no risk of overfitting as the Q^2 value is less than zero (Wang et al., 2021). In Figure 2C, the intercept value of Q^2 was −0.68, which indicated that the OPLS-DA model was reliable without overfitting. Results of PCA and OPLS-DA provided evidence that there was a remarkable difference in the lipid metabolic pattern of the laying hens in the Control group and the FLHS group.

Identification of Lipid Species and Pathway analysis

To determine the significantly changed lipid species in the liver of the FLHS group, the lipids were screened

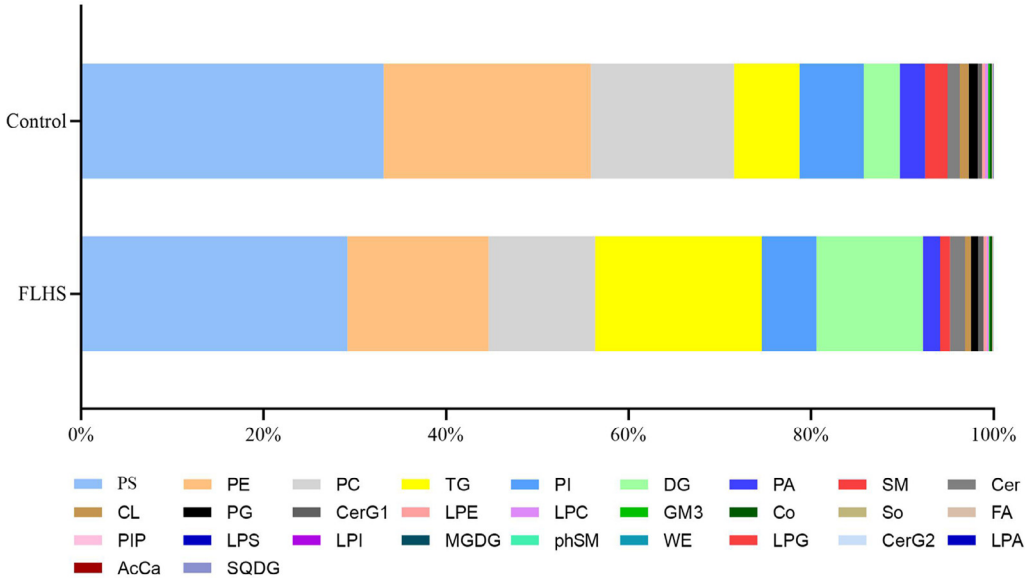

Figure 1. Stacked bar plot of differential lipid features between the Control group and the FLHS group.

based on VIP-value >1 and *P*-value (<0.05). In total, 12 lipid species with significant differences were screened out, which could be served as potential biomarkers associated with FLHS (Table 2). Compared with the Control group, the level of DG (18:1/18:1) was significantly increased in the FLHS group ($P < 0.05$), while the PE (P-16:0/18:1) ($P < 0.01$), PE (P-18:0/18:1), PE (18:0/18:1), PS (16:0/18:1), PG (18:1/18:1), PC (16:0/16:1), PS (16:0/20:4), PI (18:1/18:2), PI (18:0/20:3), cardiolipin (**CL**) (18:2/18:2/18:2/16:1), and CL (18:2/16:1/18:2/18:1) were significantly reduced ($P < 0.05$) (Figure 3A). In addition, a heatmap with hierarchical clustering analysis of the 12 individual lipid species was plotted to effectively visualize the relationship and variations in the content from different liver samples. Consistent with the results of PCA and OPLS-DA, it was found that the liver samples from the Control group and FLHS group were gathered into 2 clusters in the dendrogram of the vertical axis in the heatmap (Figure 3B). In addition, the lipid species involved in the same subclass were clustered together such as the PE, PI, and PS in the horizontal axis.

The selected lipid species were introduced to MetaboAnalyst 5.0 for pathway analysis, which could provide clues to the affected biochemical pathways that the lipids species involved. The results of the pathway analysis were shown in Figure 3C and Supplementary Table 4, and the bubble size and color represent the impact value of topology analysis and *P*-value of enrichment analysis, respectively (Jia et al., 2021). With the impact value above 0.10 and *P*-value less than 0.05, the bubbles of glycerophospholipid metabolism and linoleic acid metabolism had the largest size and the deepest color, which might be responsible for the disorders in lipid metabolism related to FLHS. Moreover, the association analysis between serum lipid parameters and lipid species was performed. In Figure 3D, it was observed that serum TG, TCH, ALT, AST, and LDL exhibited a

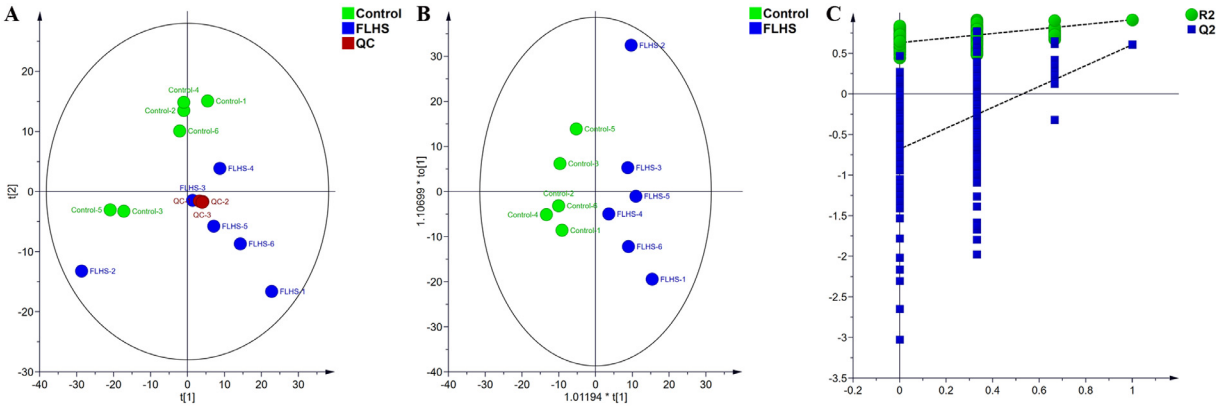

Figure 2. Analysis of the lipid profile in liver of the laying hens with FLHS. A: PCA score plots of the liver lipid profiles in the Control and FLHS groups; B: OPLS-DA score plots of the liver lipid profile in the Control and FLHS groups. The parameters of the OPLS-DA model: $R^2X = 0.60$, $R^2Y = 0.91$, and $Q^2 = 0.61$; C: Verification of the OPLS-DA model based on permutation test. The intercept of Q^2 was −0.68, indicating the robust of the OPLS-DA model.

Table 2. Identification of the differential lipid species in liver from laying hens with FLHS.

Lipid name	Formula	Ion type	m/z (measured)	RT (min)	VIP	*P*-value	FC	Trend
PE (P-16:0/18:1)	$C_{39}H_{76}O_7NP$	$[M-H]^-$	700.5287	11.75	1.46	0.0053	0.34	↓**
PE (P-18:0/18:1)	$C_{41}H_{80}O_7NP$	$[M-H]^-$	728.5600	12.76	1.17	0.0299	0.29	↓*
PE (18:0/18:1)	$C_{41}H_{80}O_8NP$	$[M-H]^-$	744.5549	12.19	3.24	0.0467	0.50	↓*
PS (16:0/18:1)	$C_{40}H_{76}O_{10}NP$	$[M-H]^-$	760.5134	10.12	1.57	0.0271	0.20	↓*
PG (18:1/18:1)	$C_{42}H_{79}O_{10}P$	$[M-H]^-$	773.5338	9.52	1.80	0.0134	0.35	↓*
PC (16:0/16:1)	$C_{40}H_{78}O_8NP$	$[M+HCOO]^-$	776.5447	10.00	1.13	0.0210	0.44	↓*
PS (16:0/20:4)	$C_{42}H_{74}O_{10}NP$	$[M-H]^-$	782.4978	9.13	1.70	0.0360	0.20	↓*
PI (18:1/18:2)	$C_{45}H_{81}O_{13}P$	$[M-H]^-$	859.5342	9.34	1.01	0.0311	0.32	↓*
DG (18:1/18:1)	$C_{39}H_{72}O_5$	$[M+NH_4]^+$	638.5718	13.00	11.21	0.0414	4.54	↑*
PI (18:0/20:3)	$C_{47}H_{85}O_{13}P$	$[M-H]^-$	887.5655	10.66	2.09	0.0441	0.13	↓*
CL (18:2/18:2/18:2/16:1)	$C_{79}H_{140}O_{17}P_2$	$[M-H]^-$	1421.9493	16.42	1.41	0.0109	0.16	↓*
CL (18:2/16:1/18:2/18:1)	$C_{79}H_{142}O_{17}P_2$	$[M-H]^-$	1423.9650	17.31	1.04	0.0225	0.13	↓*

*$P < 0.05$.
**$P < 0.01$.CL, Cardiolipin; DG, diglyceride; FC, fold change, FLHS group versus Control group; PE, phosphatidylethanolamine; PS, phosphatidylserine; PG, phosphatidylglycerol; PC, phosphatidylcholine; PI, phosphatidylinositol; RT, retention time; Trend, FLHS group versus Control group; VIP, variable importance in the projection.

positive correlation with DG (18:1/18:1), and a negative correction with the remaining 11 lipid species such as PE (P-18:0/18:1), PC (16:0/16:1), PG (18:1/18:1) and CL (18:2/18:2/18:2/16:1). In contrast, serum HDL was negatively related to the changes of DG (18:1/18:1), and positively related to the other lipid species.

Lipid Chain Unsaturation and Length Analysis

For the lipid species, the degree of unsaturation (number of double bonds) and chain length (carbon atom in the fatty acid chain) were analyzed. Compared with the Control group, it was found that the content of acyl carnitine (**AcCa**) with 1 and 2 unsaturations was significantly reduced in FLHS laying hens ($P < 0.05$) (Figure 4A). Meanwhile, lysophosphatidylserine (**LPS**) with 3 unsaturations and PE with 1 unsaturation in the liver of laying hens from FLHS group were also significantly reduced than those in the Control ($P < 0.05$). In regard to carbon chain length, the contents of AcCa at the chain lengths of 9, 14, and 18 were observed to decreased significantly in the FLHS group in comparison with Control (Figure 4B). Meanwhile, CL with the chain lengths of 66, 68, and 70, PA with chain length of 36, PE with chain length of 32, and PS with chain lengths of 32 and 34, were significantly reduced to varying degrees ($P < 0.05$ or $P < 0.01$) in the liver of laying hens with FLHS. Interestingly, these results indicated that both lipid chain unsaturation and length showed a decreased trend in the liver of the laying hens with FLHS.

In order to further study the changes in unsaturation and length of the lipid chain, the mRNA levels of CPT1, FADS1, ELOVL2, and ELOVL5 were measured (Figure 4C). Compared with the Control group, the level of ELOVL2 in the liver of the laying hens with FLHS was significantly increased ($P < 0.01$). In addition, it was observed that the mean expression levels of CPT1 and ELOVL5 were increased in the FLHS group than those in the Control, while the FADS1 was decreased, but the differences of CPT1, ELOVL5 and FADS1 were not significant.

DISCUSSION

As a metabolomic disease, FLHS is naturally occurred in old high-yield laying hens. Rozenbopm et al. found that the young hens are more sensitive to HELP diet than the old hens, that the pathological changes such as the liver fat content and liver hemorrhagic score were more obvious in the young hens than the old hens under the treatment of HELP (Rozenboim et al., 2016). In the present study, serum lipid analysis and liver histopathological examination showed increased blood lipid level and lipid deposition, which indicated the FLHS model was successfully established. In addition, the modeling method of FLHS used in this study was consistent with the previous reports (Gao et al., 2019; Zhuang et al., 2019; Xing et al., 2020). With the application of the FLHS model, the lipidomics approach was further applied to reveal the lipid perturbation in the liver of laying hens.

Liver lipid metabolism is involved in many physiological processes such as energy supply, inflammation, and cellular signaling, which plays a key role in fatty liver disease (He et al., 2020). Massive lipid hoarding is an outstanding characteristic of FLHS. To our best knowledge, the lipid metabolism in the liver from FLHS laying hens was reported in the present study with the application of LC-based lipidomics analysis for the first time. In this study, we analyzed lipid composition including lipid classes and molecular species, and investigated the changes in lipid profile in the liver from the FLHS laying hens followed by multivariate statistical analysis. In addition, the different lipid species were screened and the involved metabolic pathways were identified. More importantly, it was found that the lipid chain length and unsaturation were reduced, while the expression level of ELOVL2 was increased in the liver by FLHS. These results contributed to the understanding of the pathogenesis of FLHS from the perspective of lipid metabolism.

Many studies have demonstrated that TG is a risk factor for fatty liver disease (Ullah et al., 2019). Hepatic TG homeostasis is affected by many physiological processes such as TG synthesis, LDL secretion, and fatty

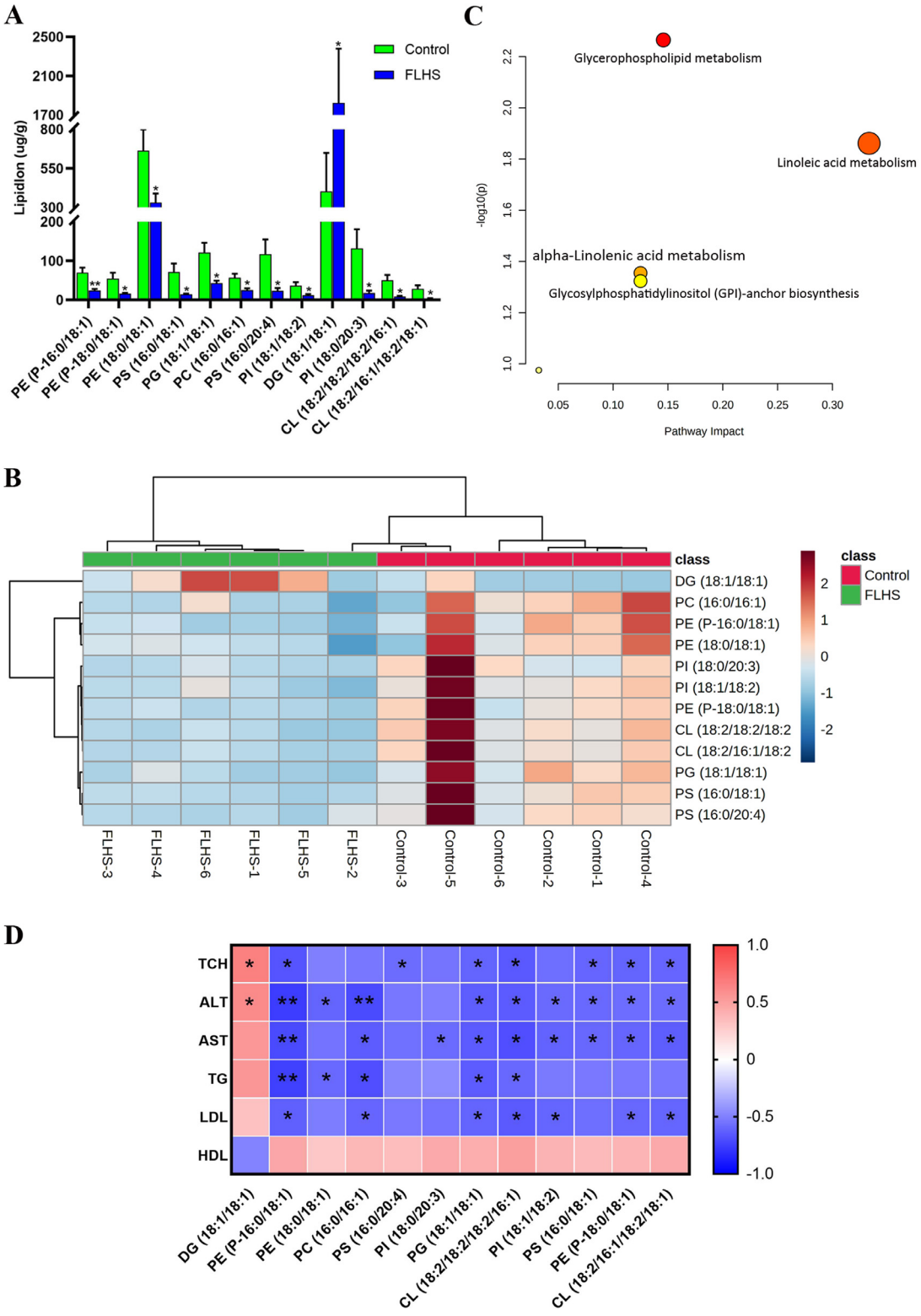

Figure 3. Quantitative measurement, heatmap and pathway analysis of the lipid species related to FLHS (n = 6). A: Quantitative measurement potential lipid species in the liver of the laying hens in the Control group and FLHS group, $^{*}P < 0.05$, $^{**}P < 0.01$. B: Hierarchical clustering heatmap of the identified lipid specie. C: Pathway analysis results of the lipid species related to FLHS. D: Spearman's correlations between serum lipid parameter and lipid species related to FLHS in laying hens. The red and blue color represent a positive or negative correlation, respectively, $^{*}P < 0.05$, $^{**}P < 0.01$.

acid uptake and oxidation (Kawano and Cohen, 2013). Miao et al. verified that the hepatic TG content was significantly increased in the laying hens with FLHS induced by the HELP diet (Miao et al., 2021). Consistent with the previous study, the lipidomics results found that the contents of TG and DG were increased in the liver of FLHS laying hens than the Control. Consumption of the HELP diet can increase fatty acid intake and further enhance lipid synthesis, which results in the accumulation of TG and DG in the liver (Choi

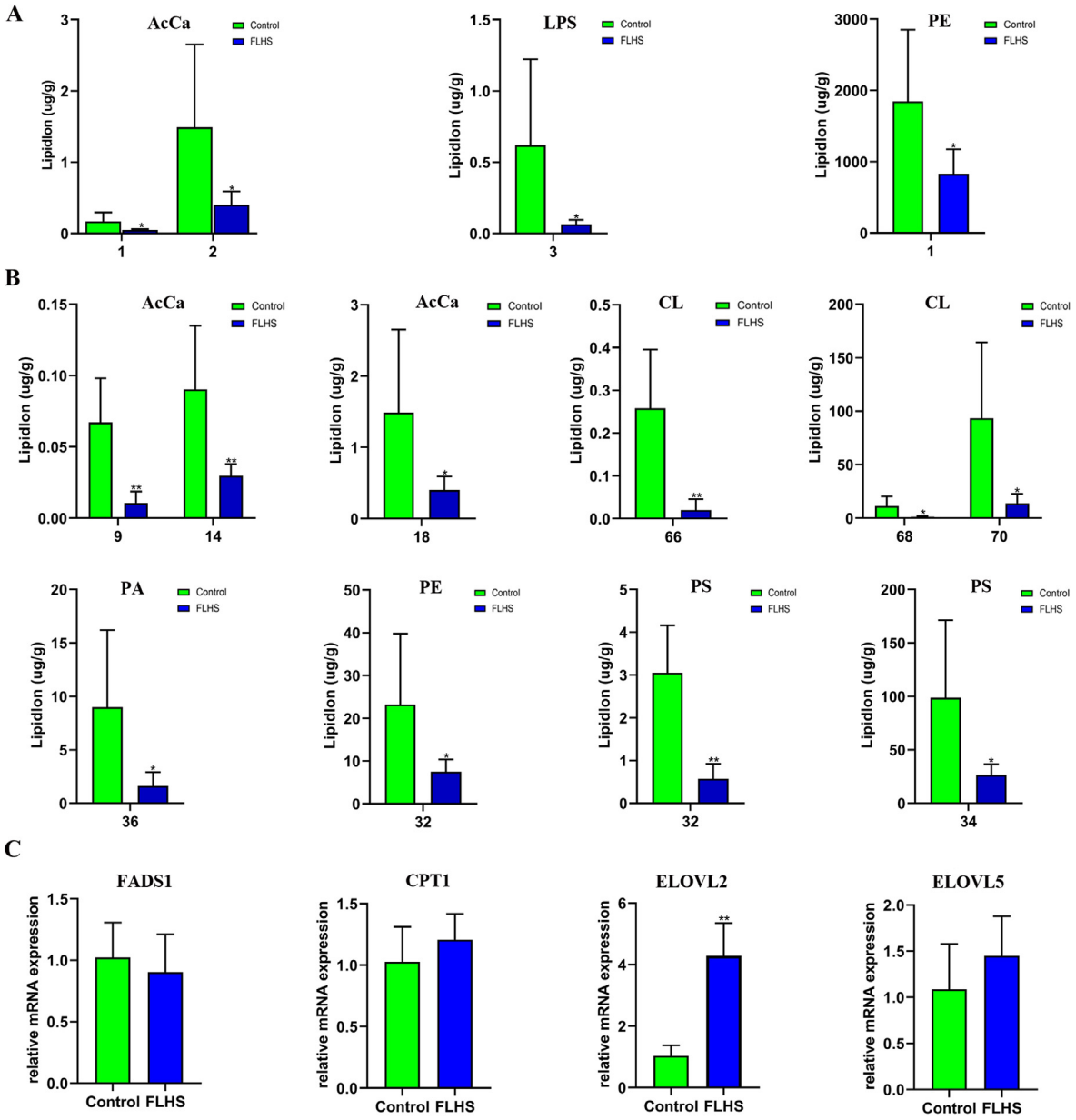

Figure 4. Changes of lipid unsaturation and lipid length in liver of FLHS laying hens (n = 6). A: Results of lipid chain unsaturation analysis. AcCa: Acyl carnitine; LPS: Lysophosphatidylserine; PE: Phosphatidylethanolamine. The X-axis indicates the degree of unsaturation, $^{*}P < 0.05$. B: Results of lipid chain length analysis. AcCa: Acyl carnitine; CL: Cardiolipin; PA: Phosphatidic acid; PE: Phosphatidylethanolamine; PS: Phosphatidylserine. The X-axis indicates the number of carbon atom, $^{*}P < 0.05$, $^{**}P < 0.01$. C: Relative expression level of FADS1, CPT1, ELOVL2 and ELOVL5, $^{**}P < 0.01$.

et al., 2012). As lipotoxic molecules, TG and DG accumulation can directly or indirectly induce metabolic stress such as oxidative stress, mitochondrial dysfunction, and insulin resistance (Ullah et al., 2019), which may be the pathogenic factors for FLHS development. It has been reported that the majority of PE, PC, and PI were decreased with the increasing severity of liver steatosis in humans (Ooi et al., 2021). Our findings were paralleled with the previous results that the levels of four glycerophospholipids including PS, PE, PC, and PE were reduced in the liver from the laying hens with FLHS. In mammalian cells, PE and PC are the most abundant glycerophospholipids. A large number of studies have suggested that inhibition of PE and PC synthesis can impair hepatic phospholipid composition, induce the disorder of energy production in mitochondria and damage the secretion of LDL. And these are closely associated with fatty liver disease (van der Veen et al., 2017). Recent studies have demonstrated that PS can improve HDL functionality, inhibit inflammation and modulate blood coagulation (Darabi and Kontush, 2016). The decreased levels of PS, PE, PC and PE in liver samples of FLHS laying hens suggested that the glycerophospholipid metabolism was down-regulated, which might be involved in the pathogenesis of FLHS.

In the present study, the PCA and OPLS-DA score plots revealed that the lipid profile of FLHS laying hens was differed from those in the Control, which suggested that the lipid profiles were profoundly affected by the HELP diet. Furthermore, the liver lipidomic analysis

identified 12 lipid species including 3 PEs, 2 PSs, 2 CLs, 2 PIs, 1 PG, 1 DG as well as 1 PC. The pathway analysis revealed that the metabolism of glycerophospholipid and linoleic acid were altered with FLHS. Investigation of the content changes of these lipid species and their biological function can assist in revealing the pathogenesis of FLHS in laying hens.

By the action of diglyceride acyltransferase, DG is converted to TG through the addition of fatty acid (Greene et al., 2015). It was noted that the level of DG (18:1/18:1) in FLHS laying hens was 4.54-fold higher than the Control, which might be responsible for the TG accumulation in the liver. In addition, the soybean oil used in this experiment is rich in polyunsaturated fatty acid (PUFA). Tian et al. found that PUFA could significantly increase the level of TG in the mice liver (Tian et al., 2018). Therefore, the high PUFA diet also might be one of the reasons for the increase of TG. As a mitochondrial specific phospholipid, the decline of CL can lead to mitochondrial dysfunction and impair the activities of carrier proteins in the electron transport chain, resulting in the reduced production of ATP (Gasanoff et al., 2021). In this study, CL (18:2/18:2/18:2/16:1) and CL (18:2/16:1/18:2/18:1) were significantly reduced in the liver from FLHS laying hens, which suggested the disorder of energy metabolism was accompanied by the pathogenesis of FLHS. In accordance with the decreasing tendencies of PEs and PC found in the present study, Feng et al. observed that the levels of PE and PC species were significantly lower in the liver of mice fed with a high-fat western-style diet than those in the control group (Feng et al., 2018). It is well known that PI is a key cell membrane constituent, and as the primary source can be metabolized into arachidonic acid by the enzyme phospholipase A2. In our previous study, we found that the arachidonic acid metabolism was disturbed that the concentration of arachidonic acid was reduced in the liver in laying hens with FLHS (Meng et al., 2021). Therefore, it was speculated that the reduction of PI (18:1/18:2) and PI (18:0/20:3) might contribute to the arachidonic acid decrease, which provided evidence for understanding the metabolic imbalance of arachidonic acid in the pathogenesis of FLHS. Moreover, as the main component phospholipid of cell membrane, insufficient synthesis of PI, PS, PE, and PC can damage the membrane integrity of hepatocyte, which is tightly linked to the pathogenesis of FLHS (Chiappini et al., 2017).

Lipid unsaturation degree and chain length can affect the mechanical properties of cell membrane such as fluidity and thickness. It is involved in the process of inflammation, oxidation, and energy production. Several studies have proved that desaturation and elongation of fatty acids are the pathogenesis of NAFLD (Notarnicola et al., 2017; Li et al., 2022). Through the lipidomic analysis, we observed that the chain unsaturation and length of lipid species were reduced in the liver from FLHS laying hens, suggesting that the alterations in the lipid structure were potential causes for FLHS.

It has been reported that the fatty acid β-oxidation was impaired and decreased in laying hens with FLHS (Miao et al., 2021). CTP1 is the rate-limiting enzyme of fatty acid oxidation, which regulates the entry progress of fatty acid into mitochondria. Gao et al. reported that CPT1 was significantly down-regulated in the liver of 450-day-old Hy-Line Brown laying hens feeding with HELP for 90 d (Gao et al., 2021). However, no significance of CTP1 was observed in the present study, which might be caused by animal age, the HELP consumption time and the metabolic energy provided by the diets. As the essential enzyme in polyunsaturated fatty acid production, FADS1 was demonstrated to be decreased in liver disease such as NAFLD (Li et al., 2020). The expression of FADS1 in the FLHS group had a decreasing tendency, which might be one of the reasons for the decreased degree of fatty acid unsaturation in the FLHS group. ELOVL2 and ELOVL5 are highly expressed in the liver of laying hens (Gregory et al., 2013), and participate in the extension of long chain fatty acid. In a previous study, it was reported that a high fat diet feeding could induce high expression of ELOVL2 in the liver of C57BL/6 mice both at mRNA and protein levels (Zhou et al., 2018). Consistent with the previous study, we found that the FLHS laying hens showed significantly increased ELOVL2 level in the liver than the Control. However, the result of ELOVL2 was discrepant from the findings by the lipidomics analysis that the lipid chain length was reduced by FLHS. Lipid unsaturation and chain length are affected by many biological factors such as lipid metabolic enzymes and lipid saturation receptors (Wang et al., 2006), and more in-depth research is needed to explore the mechanism of changes in lipid unsaturation and chain length related to FLHS.

The strength of the present study is that UHPLC Q-Exactive MS based deep and comprehensive liver lipidomic analysis provides an overview of liver lipidome in laying hens. The pathogenesis in FLHS was explored by the lipidomics method for the first time. As a pilot study, it was important to note that the small sample size was the limitation of the present work. However, significant changes in lipid profile were found in FLHS laying hens even with a small number of liver samples, which need to be further evaluated and verified in more studies with large sample capacities. In addition, the lipid profile of FLHS laying hens in this study was not related to other pathogenic factors of FLHS such as inflammation, oxidative stress, and cell apoptosis. To date, there have been very few studies about the detailed biological function of the particular lipid species. Therefore, an integrative and systematic study of the role of lipids may facilitate the understanding of the pathophysiology of FLHS in laying hens.

In conclusion, the global lipid profile in the liver associated with FLHS was investigated with the application of LC-MS based lipidomics approach. In this study, 29 different lipid subclasses including 1302 lipid species were identified. Different lipid composition changes in the liver, such as increased levels of DG and TG, and the decrease of PS, PE, PC and PI, may be related to FLHS or the high PUFA diet. The lipid profile was also altered in the liver in FLHS laying hens, and 12 potential lipid

species were found to explain the pathogenesis of FLHS. Furthermore, lipid chain length and unsaturation degree were found to be reduced by FLHS. This study provides new insights for understanding the role of lipid metabolism in FLHS, and also suggests that lipidomics was a powerful tool to explore the pathogenesis of FLHS.

ACKNOWLEDGMENTS

This work was supported by Natural Science Foundation of Hebei Province (C2021204035) and Hebei Key Technology R&D Program (22326619D), and the Hebei Layer and Broiler Innovation Team of Modern Argo-industry Technology Research System (HBCT2018150210). We are grateful for the technical support of Shanghai Applied Protein Technology Co. Ltd in lipidomic analysis.

DISCLOSURES

The authors declare no conflict of interest.

SUPPLEMENTARY MATERIALS

Supplementary material associated with this article can be found in the online version at doi:10.1016/j.psj.2022.102352.

REFERENCES

Cheng, X., J. Liu, Y. Zhu, X. Guo, P. Liu, C. Zhang, H. Cao, C. Xing, Y. Zhuang, and G. Hu. 2022. Molecular cloning, characterization, and expression analysis of TIPE1 in chicken (Gallus gallus): Its applications in fatty liver hemorrhagic syndrome. Int. J. Biol. Macromol. 207:905–916.

Chiappini, F., A. Coilly, H. Kadar, P. Gual, A. Tran, C. Desterke, D. Samuel, J. C. Duclos-Vallée, D. Touboul, J. Bertrand-Michel, A. Brunelle, C. Guettier, and F. Le Naour. 2017. Metabolism dysregulation induces a specific lipid signature of nonalcoholic steatohepatitis in patients. Sci. Rep. 7:46658.

Choi, Y. I., H. J. Ahn, B. K. Lee, S. T. Oh, B. K. An, and C. W. Kang. 2012. Nutritional and hormonal induction of fatty liver syndrome and effects of dietary lipotropic factors in egg-type male chicks. Asian-Australas. J. Anim. Sci. 25:1145–1152.

Darabi, M., and A. Kontush. 2016. Phosphatidylserine in atherosclerosis. Curr. Opin. Lipidol. 27:414–420.

Ding, M., and K. M. Rexrode. 2020. A review of lipidomics of cardiovascular disease highlights the importance of isolating lipoproteins. Metabolites. 10:163.

Emwas, A. H., R. Roy, R. T. McKay, L. Tenori, E. Saccenti, G. Gowda, D. Raftery, F. Alahmari, L. Jaremko, M. Jaremko, and D. S. Wishart. 2019. NMR spectroscopy for metabolomics research. Metabolites. 9:123.

Eylem, C. C., T. Reçber, M. Waris, S. Kır, and E. Nemutlu. 2022. State-of-the-art GC-MS approaches for probing central carbon metabolism. Microchem. J. 172:106892.

Feng, S., Z. Dai, A. B. Liu, J. Huang, N. Narsipur, G. Guo, B. Kong, K. Reuhl, W. Lu, Z. Luo, and C. S. Yang. 2018. Intake of stigmasterol and β-sitosterol alters lipid metabolism and alleviates NAFLD in mice fed a high-fat western-style diet. Biochim. Biophys. Acta Mol. Cell Biol. Lipids. 1863:1274–1284.

Feng, K., Y. Lan, X. Zhu, J. Li, T. Chen, Q. Huang, C. T. Ho, Y. Chen, and Y. Cao. 2020. Hepatic lipidomics analysis reveals the antiobesity and cholesterol-lowering effects of tangeretin in high-fat diet-fed rats. J. Agric. Food Chem. 68:6142–6153.

Gao, X., S. Liu, C. Ding, Y. Miao, Z. Gao, M. Li, W. Fan, Z. Tang, N. H. Mhlambi, L. Yan, and S. Song. 2021. Comparative effects of genistein and bisphenol A on non-alcoholic fatty liver disease in laying hens. Environ. Pollut. 288:117795.

Gao, X., P. Liu, C. Wu, T. Wang, G. Liu, H. Cao, C. Zhang, G. Hu, and X. Guo. 2019. Effects of fatty liver hemorrhagic syndrome on the AMP-activated protein kinase signaling pathway in laying hens. Poult. Sci. 98:2201–2210.

Gasanoff, E. S., L. S. Yaguzhinsky, and G. Garab. 2021. Cardiolipin, non-bilayer structures and mitochondrial bioenergetics: relevance to cardiovascular disease. Cells. 10:1721.

Gika, H. G., I. D. Wilson, and G. A. Theodoridis. 2014. LC-MS-based holistic metabolic profiling. Problems, limitations, advantages, and future perspectives. J. Chromatogr. B Analyt. Technol. Biomed. Life Sci. 966:1–6.

Greene, D. J., L. Izem, and R. E. Morton. 2015. Defective triglyceride biosynthesis in CETP-deficient SW872 cells. J. Lipid Res. 56:1669–1678.

Gregory, M. K., M. S. Geier, R. A. Gibson, and M. J. James. 2013. Functional characterization of the chicken fatty acid elongases. J. Nutr. 143:12–16.

He, J., P. Zhang, L. Shen, L. Niu, Y. Tan, L. Chen, Y. Zhao, L. Bai, X. Hao, X. Li, S. Zhang, and L. Zhu. 2020. Short-chain fatty acids and their association with signalling pathways in inflammation, glucose and lipid metabolism. Int. J. Mol. Sci. 21:6356.

Jia, W., R. Li, X. Wu, S. Liu, and L. Shi. 2021. UHPLC-Q-Orbitrap HRMS-based quantitative lipidomics reveals the chemical changes of phospholipids during thermal processing methods of Tan sheep meat. Food Chem. 360:130153.

Kawano, Y., and D. E. Cohen. 2013. Mechanisms of hepatic triglyceride accumulation in non-alcoholic fatty liver disease. J. Gastroenterol. 48:434–441.

Li, J., T. Vosegaard, and Z. Guo. 2017. Applications of nuclear magnetic resonance in lipid analyses: An emerging powerful tool for lipidomics studies. Prog. Lipid Res. 68:37–56.

Li, Y., C. Wang, Y. Jin, H. Chen, M. Cao, W. Li, H. Luo, and Z. Wu. 2020. Huang-Qi San improves glucose and lipid metabolism and exerts protective effects against hepatic steatosis in high fat diet-fed rats. Biomed. Pharmacother. 126:109734.

Li, P., R. Zhang, M. Wang, Y. Chen, Z. Chen, X. Ke, L. Zuo, and J. Wang. 2022. Baicalein prevents fructose-induced hepatic steatosis in rats: In the regulation of fatty acid de novo synthesis, fatty acid elongation and fatty acid oxidation. Front. Pharmacol. 13:917329.

Liu, H., T. Chen, X. Xie, X. Wang, Y. Luo, N. Xu, Z. Sa, M. Zhang, Z. Chen, X. Hu, and J. Li. 2021. Hepatic lipidomics analysis reveals the ameliorative effects of highland barley β-Glucan on Western diet-induced nonalcoholic fatty liver disease mice. J. Agric. Food Chem. 69:9287–9298.

Matyash, V., G. Liebisch, T. V. Kurzchalia, A. Shevchenko, and D. Schwudke. 2008. Lipid extraction by methyl-tert-butyl ether for high-throughput lipidomics. J. Lipid Res. 49:1137–1146.

Meikle, P. J., G. Wong, C. K. Barlow, and B. A. Kingwell. 2014. Lipidomics: potential role in risk prediction and therapeutic monitoring for diabetes and cardiovascular disease. Pharmacol. Ther. 143:12–23.

Meng, J., N. Ma, H. Liu, J. Liu, J. Liu, J. Wang, X. He, and X. Zhao. 2021. Untargeted and targeted metabolomics profiling reveals the underlying pathogenesis and abnormal arachidonic acid metabolism in laying hens with fatty liver hemorrhagic syndrome. Poult. Sci. 100:101320.

Miao, Y. F., X. N. Gao, D. N. Xu, M. C. Li, Z. S. Gao, Z. H. Tang, N. H. Mhlambi, W. J. Wang, W. T. Fan, X. Z. Shi, G. L. Liu, and S. Q. Song. 2021. Protective effect of the new prepared Atractylodes macrocephala Koidz polysaccharide on fatty liver hemorrhagic syndrome in laying hens. Poult. Sci. 100:938–948.

Notarnicola, M., M. G. Caruso, V. Tutino, C. Bonfiglio, R. Cozzolongo, V. Giannuzzi, V. De Nunzio, G. De Leonardis, D. I. Abbrescia, I. Franco, V. Intini, A. Mirizzi, and A. R. Osella. 2017. Significant decrease of saturation index in erythrocytes membrane from subjects with non-alcoholic fatty liver disease (NAFLD). Lipids Health Dis. 16:160.

Ooi, G. J., P. J. Meikle, K. Huynh, A. Earnest, S. K. Roberts, W. Kemp, B. L. Parker, W. Brown, P. Burton, and M. J. Watt. 2021. Hepatic lipidomic remodeling in severe obesity

manifests with steatosis and does not evolve with non-alcoholic steatohepatitis. J. Hepatol. 75:524–535.

Pang, Z., G. Zhou, J. Ewald, L. Chang, O. Hacariz, N. Basu, and J. Xia. 2022. Using MetaboAnalyst 5.0 for LC-HRMS spectra processing, multi-omics integration and covariate adjustment of global metabolomics data. Nat. Protoc. 17:1735–1761.

Puri, P., R. A. Baillie, M. M. Wiest, F. Mirshahi, J. Choudhury, O. Cheung, C. Sargeant, M. J. Contos, and A. J. Sanyal. 2007. A lipidomic analysis of nonalcoholic fatty liver disease. Hepatology. 46:1081–1090.

Rozenboim, I., J. Mahato, N. A. Cohen, and O. Tirosh. 2016. Low protein and high-energy diet: a possible natural cause of fatty liver hemorrhagic syndrome in caged White Leghorn laying hens. Poult. Sci. 95:612–621.

Shini, A., S. Shini, and W. L. Bryden. 2019. Fatty liver haemorrhagic syndrome occurrence in laying hens: impact of production system. Avian Pathol. 48:25–34.

Tian, F., J. Wang, H. Sun, J. Yang, P. Wang, S. Wan, X. Gao, L. Zhang, J. Li, and X. Wang. 2018. N-3 polyunsaturated fatty acids ameliorate hepatic steatosis via the PPAR-α/CPT-1α pathway in a mouse model of parenteral nutrition. Biochem. Bioph. Res. Co. 501:974–981.

Ullah, R., N. Rauf, G. Nabi, H. Ullah, Y. Shen, Y. D. Zhou, and J. Fu. 2019. Role of nutrition in the pathogenesis and prevention of non-alcoholic fatty liver disease: recent updates. Int. J. Biol. Sci. 15:265–276.

van der Veen, J. N., J. P. Kennelly, S. Wan, J. E. Vance, D. E. Vance, and R. L. Jacobs. 2017. The critical role of phosphatidylcholine and phosphatidylethanolamine metabolism in health and disease. Biochim. Biophys. Acta. Biomembr. 1859:1558–1572.

Wang, Y., D. Botolin, J. Xu, B. Christian, E. Mitchell, B. Jayaprakasam, M. G. Nair, J. M. Peters, J. V. Busik, L. K. Olson, and D. B. Jump. 2006. Regulation of hepatic fatty acid elongase and desaturase expression in diabetes and obesity. J. Lipid Res. 47:2028–2041.

Wang, Z. H., K. I. Zheng, X. D. Wang, J. Qiao, Y. Y. Li, L. Zhang, M. H. Zheng, and J. Wu. 2021. LC-MS-based lipidomic analysis in distinguishing patients with nonalcoholic steatohepatitis from nonalcoholic fatty liver. Hepatobiliary Pancreat. Dis. Int. 20:452–459.

Xing, C., Y. Wang, X. Dai, F. Yang, J. Luo, P. Liu, C. Zhang, H. Cao, and G. Hu. 2020. The protective effects of resveratrol on antioxidant function and the mRNA expression of inflammatory cytokines in the ovaries of hens with fatty liver hemorrhagic syndrome. Poult. Sci. 99:1019–1027.

Yang, L., M. Li, Y. Shan, S. Shen, Y. Bai, and H. Liu. 2016. Recent advances in lipidomics for disease research. J. Sep. Sci. 39:38–50.

Zhou, Y., Y. Ding, J. Zhang, P. Zhang, J. Wang, and Z. Li. 2018. Alpinetin improved high fat diet-induced non-alcoholic fatty liver disease (NAFLD) through improving oxidative stress, inflammatory response and lipid metabolism. Biomed. Pharmacother. 97:1397–1408.

Zhuang, Y., C. Xing, H. Cao, C. Zhang, J. Luo, X. Guo, and G. Hu. 2019. Insulin resistance and metabonomics analysis of fatty liver haemorrhagic syndrome in laying hens induced by a high-energy low-protein diet. Sci. Rep. 9:10141.